Optical Materials 119 (2021) 111304

Contents lists available at ScienceDirect

Optical Materials

journal homepage: www.elsevier.com/locate/optmat

Research Article

Effect of 130 keV pulsed electron irradiation on the efficiency of radiative transitions in Eu-doped glass-ceramics $CaSiO_3$

Carlos D. Gonzales-Lorenzo [a,d,*], D.V. Ananchenko [b], S.V. Nikiforov [b], A.N. Kiryakov [b], A. F. Zatsepin [b], Jose F.D. Chubaci [a], N.F. Cano [c], Jorge S. Ayala-Arenas [d], Shigueo Watanabe [a]

[a] Instituto de Física, Universidade de São Paulo, Rua Do Matão, Travessa R, 187, CEP, 05508-090, São Paulo, SP, Brazil
[b] Ural Federal University, Ulitsa Mira, 21, Ekaterinburg, Russia
[c] Instituto Do Mar, Universidade Federal de São Paulo, Rua. Doutor Carvalho de Mendonça, 144, CEP, 11070-100, Santos, SP, Brazil
[d] Escuela Profesional de Física, Facultad de Ciencias Naturales y Formales, Universidad Nacional de San Agustín (UNSA), Av. Independencia S/N, Arequipa, Peru

ARTICLE INFO

Keywords:
Glass-ceramics
Pseudowollastonite $CaSiO_3$
Eu^{3+} photoluminescence
Electron beam irradiation
Optical material

ABSTRACT

Polycrystalline glass-ceramic $CaSiO_3$ doped with Eu^{3+} ions was obtained by devitrification. The analysis of the photoluminescent characteristics of the obtained glass-ceramic is carried out. It was found that as a result of the devitrification of $CaSiO_3$, two phases are formed, identified as pseudowollastonite (β-$CaSiO_3$) as the dominant phase together with a small percentage of tridymite (SiO_2). The UV–Vis optical absorption of Eu^{3+}-doped $CaSiO_3$ was performed using a UV–Vis spectrophotometer. The main objective of this work was to study the effect of the pulsed corpuscular action of electrons accelerated in a field of 130 keV on energy transitions in the Eu^{3+} ion. It is found that, upon steady-state excitation of the photoluminescent signal in the PLE spectra of unirradiated samples at wavelengths below 300 nm, two broad excitation peaks are displayed, possibly associated with O − Eu and O − Si CT transitions. Above 300 nm the characteristic excitation band from $^7F_0$ ground state to ^5H_j, $^5D_4$, ^5G_j, $^5L_6$, $^5D_3$, and $^5D_2$ states of the Eu^{3+} ions are shown. It was found that, as a result of exposure to an electron beam in the photoluminescence spectra of europium, a redistribution of the relative intensities of the $^5D_0 \rightarrow {}^7F_2$ and $^5D_0 \rightarrow {}^7F_1$ transitions occurs. The calculation of the asymmetry ratio of these transitions showed values for an unirradiated sample $R_{21} = 2.06$ and irradiated $R_{21} = 2.52$, which indicates a decrease in the symmetry of the crystal field around Eu^{3+} ions after irradiation. Several reasons for the decrease in the relative intensity of the Eu^{3+} luminescence signal after electron irradiation, caused by the effect of electrization of the material, intrinsic defects of the matrix, and inhomogeneous phase composition, are discussed.

1. Introduction

Luminescent glass-ceramics are being actively investigated due to their increased functional characteristics in comparison with conventional glasses. The interest in materials of this type is due to their composite structure, which combines the advantages of both glasses and crystals. The presence of crystal grains in glass-ceramics provides a solution to several important problems at once: firstly, such material is mechanically more durable, secondly, it has increased resistance to high-energy impact, thirdly, ions activators of rare earth (RE) localized in the crystal structure are limited by phonons with lower energies, which increases the lifetimes in the excited state and the absorption cross-section of excitation photons in comparison with glassy media [1–3]. The corpuscular effect on glass ceramics makes it possible to modify its optical properties [4–7], but the mechanisms of such changes have not been fully established.

The investigation of radiation effects over several materials has been the subject of many studies in the past [8–11]. Radiation can induce and/or create new defects in luminescence materials modifying their optical absorption and stimulated emission properties [9–11]. Very often luminescent materials are used whenever high radiation is involved like in preservation of food by high dose radiation, or in experiments with charged particles accelerated by high electric potential, or in a reactor in operation. Therefore, it is essential to investigate the effects of radiation on such materials. Several solid materials have been investigated such as rare earth doped solids [12–15]. Also, natural

* Corresponding author. Instituto de Física, Universidade de São Paulo, Rua do Matão, Travessa R, 187, CEP, 05508-090, São Paulo, SP, Brazil.
E-mail addresses: clorenzo@if.usp.br (C.D. Gonzales-Lorenzo), d.v.ananchenko@urfu.ru (D.V. Ananchenko), s.v.nikiforov@urfu.ru (S.V. Nikiforov), arseny.kiriakov@urfu.ru (A.N. Kiryakov), a.f.zatsepin@urfu.ru (A.F. Zatsepin), watanabe@if.usp.br (S. Watanabe).

https://doi.org/10.1016/j.optmat.2021.111304
Received 29 May 2021; Accepted 21 June 2021
Available online 28 June 2021

minerals, particularly silicate minerals [16–19]; have been considered. Then one finds other compounds as hosts for rare-earths, such as oxides [10], sulfates [14], borates, and vanadates [9,11,12,20]. When rare-earth ions are mixed with luminescent materials, these compounds show interesting properties whose application in luminescence and display technologies have been the subject of study in physics and chemistry areas. Among the rare-earth used, Eu, Sm, and Yb have driven special attention because it exhibits two possible valence states, divalent as well as trivalent states [19]. For Eu^{3+}, for example, the electron configuration of Eu^{3+} ions is $4f^6$ which is characterized by the f transition in the red region of the luminescence spectra [16,21,22]. Particularly, Eu^{3+} doped solid-state materials have been broadly used in color television, plasma display panels (PDP), cathode ray tube, high-efficiency fluorescent lamps, waveguides, and light-emitting diode due to their outstanding photoluminescence (PL) properties [12,13,18,23].

For this reason, luminescence studies of europium have been extensively carried out in different host materials produced by different methods. Pandey et al. ([14]) have produced nanocrystalline $K_2Ca_2(SO_4)_3$:Eu prepared by co-precipitation method and their thermoluminescence (TL) and photoluminescence (PL) studied. They have found two overlapping broad peaks around 400 and 450 nm in the emission spectra which could be due to Eu^{2+} emission. Trinh et al. ([20]) have produced powders of nanocrystalline YVO_4:Eu^{3+} by a wet chemical method where PL results display a strongest red emission peak at the wavelength around 618 nm. Niraula et al. ([13]) have synthesized Eu^{3+} doped $CaSiO_3$ Nano-phosphor of different grain sizes by the microemulsion technique. They have shown that the PL intensity always increased with decreasing grain sizes of this crystalline powder. Furthermore, the devitrification method is another known method for the production of polycrystalline materials [24–26]. The advantage of this method is due to the relatively easy production of polycrystals without the need for sophisticated equipment and the greater amount of material obtained compared to other methods. These features are important when larger-scale production is required.

On the other hand, luminescence spectra after ionizing radiation of these Eu^{3+} doped luminescence materials have been studied by several authors [9,11,14,27]. It has been observed that irradiation with ionizing radiation of these materials may change the valence state of the dopant by oxidation-reduction or ionization process and producing or creating defect centers (such as F-center), recombination center, traps, and absorption bands in the crystal lattice [28,29]. Pulsed electron beams with the electron energy of 100–300 keV is one of the types of high-dose irradiation used in electronic industry and in radiation physics to know the radiation effect on luminescence materials [30].

Silicate as a host of europium has been considered as one of the best materials for luminescence centers due to its chemical and thermal stability [16,21,22]. Calcium silicate, for example, has been broadly studied in the past years for several authors as an interesting host for Eu^{3+} displaying notable luminescence spectra in the red region [16–18,22,31].

No work has been reported about the effect of electron radiation on luminescence properties in Eu doped $CaSiO_3$ phosphor. In this work, we show our first results about the pulsed electron beam irradiation effect on the photoluminescence characteristics of the polycrystalline glass-ceramic $CaSiO_3$ doped with Eu^{3+} ions, produced by the devitrification method, seeing its possible applications in the electronics industry.

2. Experimental details

Synthetic polycrystalline glass-ceramic Eu doped $CaSiO_3$ was produced by the devitrification method [25,26]. In this work, we used 12.0 g (44.4 wt %) CaO (Anidrol-PA ACS, 99.9%) and 15.0 g (55.6 wt %) of SiO_2 and the starting materials were mixed. After that, an appropriate quantity of Eu_2O_3 (Sigma Aldrich/PA ACS, 99.9999%) was used to obtain an amount of 1000 ppm of Eu as dopant on the CaO–SiO_2 mixture. Finally, the mixture with the dopant is then placed in an oven heated to 1500 °C to melt the above mixture, for 2 h in an ambient atmosphere. The melt is then cooled slowly using a temperature controller so that the room temperature is reached after about 24 h.

This polycrystalline sample of $CaSiO_3$:Eu was crushed and sieved to obtain grains smaller than 0.075 mm in diameter to be used in the structural analysis by X-rays diffraction (XRD) method. XRD data of powder sample at room temperature were obtained on Rigaku Miniflex 300 diffractometer with Cu $K_{\alpha 1}$ (0.15406 nm) radiation between 10° and 60° at a 0.02° (in 2θ) scanning step and a 1 s step time.

Besides, this powder was placed in a sealed container together with two milling alumina spheres. Then, the container is left in a mill for 24 h to homogenize and reduce the particle size of the sample. Later, 100 mg of the powder obtained after the homogenizing process was used to produce pellets of about 6 mm in diameter and 1 mm thick. For this purpose, this powder was subjected to a pressure of 800 kgf/cm^2 using a mechanical press. After that, the resulted pellets of 6 mm in diameter and 1 mm thick were sintered at 900 °C for 3 h.

Some of these pellets of $CaSiO_3$:Eu were irradiated at room temperature to a pulsed electron beam of RADAN accelerator at the Institute of Physics and Technology of the Ural Federal University (UrFU), with a pulse duration of 2 ns, mean electron energy 130 ± 1 keV, current density 60 A/cm^2, and mean absorbed dose of 1.5 kGy/pulse.

Spectrometer LS-55 from (from UrFU) was used for photoluminescence measurements and the result was recorded at room temperature. A 150 W xenon lamp, which works in pulses mode, was used to excite PL. The light emission was detected by R928 photomultiplier tube that has a wavelength range from 200 to 900 nm and maximal sensitivity at about 400 nm. The UV-VIS spectroscopy measurement has been performed on a Shimadzu-2600 UV–Visible spectrophotometer at the National Engineering University (UNI), Peru.

3. Results and discussion

3.1. X-ray diffraction studies

The diffractogram of the $CaSiO_3$:Eu synthetic material is shown in

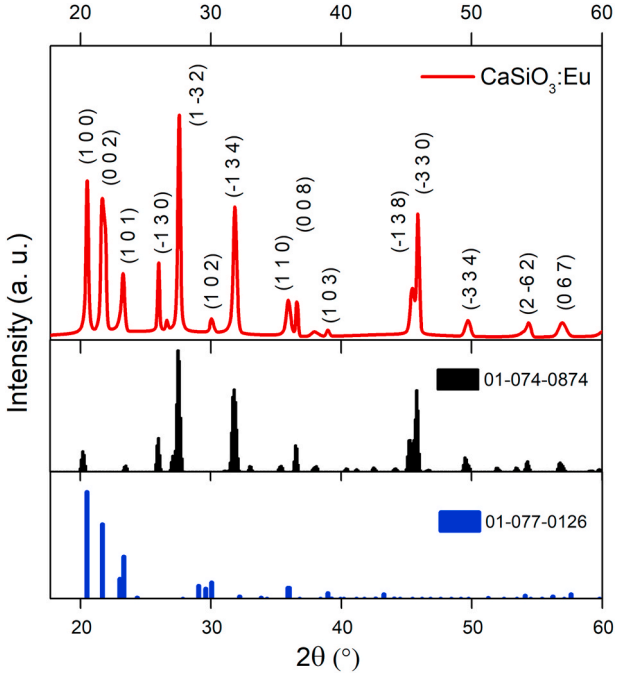

Fig. 1. XRD pattern of $CaSiO_3$:Eu produced in this work, compared with XRD patterns from PDF-2 files: 01-074-0874 (pseudowollastonite) and 01-077-0126 (tridymite) - X'Pert HighScore program [32].

Fig. 1. All the diffraction peaks in the spectrum are coincident to the pseudowollastonite (β-$CaSiO_3$) crystal pattern and tridymite (polymorphic of quartz - SiO_2).

Both phases are matched with 01-074-0874 and 01-077-0126 PDF-2 files of the X'Pert HighScore Plus software [32] for pseudowollastonite (β-$CaSiO_3$) and tridymite (polymorphic of quartz - SiO_2), respectively. This software was used for the refinement and to determine the percentage of each crystalline phase in the sample. The results have shown that 91% of the sample is belonging to pseudowollastonite and 9% to tridymite. In this way, β-$CaSiO_3$ type polycrystalline structure dominates this sample.

Pseudowollastonite phase found in this material is referred to that found by Yamanaka and Mori ([33]). They have identified the presence of at least three polytypes structures of β-$CaSiO_3$. These are the four-layer, six-layer, and disordered stacking polytypes. The structure of the four-layer polytype is the dominant phase with a triclinic unit cell and solved in space group $C\bar{1}$. The crystal data of this structure were found to be: Z = 24, a = 6.853 (3), b = 11.895 (5), c = 19.674 (13)A, α = 90.12 (3), β = 90.55 (3), γ = 90.00 (3)°. Besides, this structure is formed for four Ca-octahedra layers and ternary rings of three tetrahedra of Si_3O_9 interposed between the layers. These Ca-octahedra in a layer are compressed in the c-direction, while tetrahedra of the rings are elongated in the same direction (stacking direction). Fig. 2 shows the stacking sequence of layers for the four-layer polytype structure with ternary rings of three tetrahedra in gray, Ca^{2+} ion in purple, and O^{2-} ion in red. The six-layer polytype has been indicated as having a pseudo-symmetry C2/c and is probably isostructural with SrGeO3. Finally, the disordered structure was confirmed by diffuse streaks along c* axis with the presence of many polytypes along c axis [33].

3.2. Photoluminescence and absorption studies

The UV–Vis optical absorption of polycrystalline glass-ceramic Eu^{3+}-doped $CaSiO_3$ was performed using a UV–Vis spectrophotometer. Fig. 3 shows the optical absorption spectra of the Eu doped $CaSiO_3$ structure. This spectrum shows an intense absorption band between 200

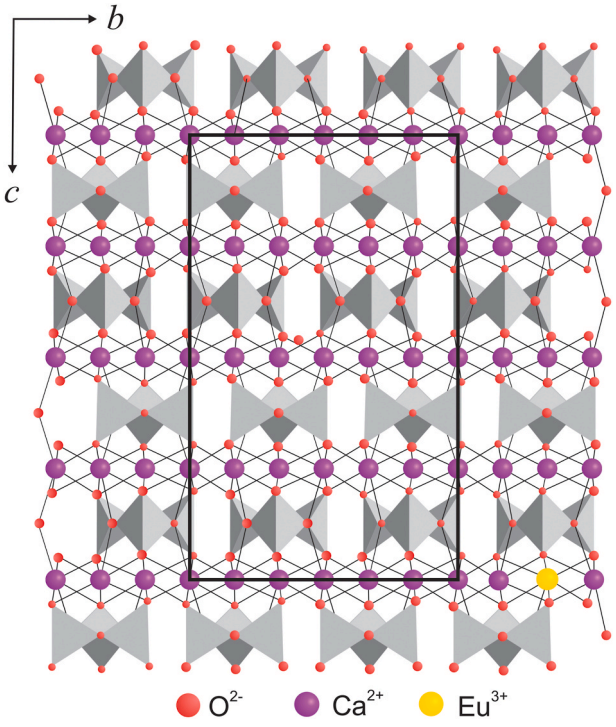

Fig. 2. Stacking sequence of layers of (Si_3O_9) rings in four-layer pseudowollastonite polytype. After [34].

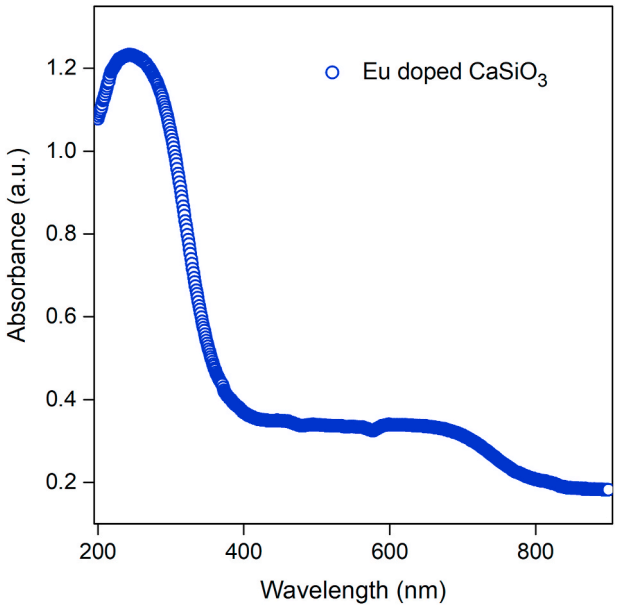

Fig. 3. UV–Vis absorption spectra of Polycrystalline glass-ceramic $CaSiO_3$ doped with Eu^{3+} ions (1000 ppm).

to 300 nm which is attributed to the oxygen to silicon (O–Si) ligand to metal charge-transfer (LMCT) in the SiO_4^{2-} group. Whilst the broad-band between 300 to 500 is attributed to the intra configurational 4f →4f transitions from the $^7F_0$ level (excitation spectra) [21,23]. The formation of the induced broad visible band could be attributed to the formation of a silicon-oxygen hole center (SiOHC) or nonbridging oxygen hole center (NBOHC) as suggested by ElBatal et al. ([35]). Beyond the range of the visible region, no further optical absorption bands are identified.

According to Yamanaka and Mori ([33]), in the four-layer polytype structure of β-$CaSiO_3$, Ca is coordinated with eight O atoms. Accordingly, ionic radii of Ca^{2+} and Eu^{3+} are 1.12 nm and 1.066 respectively [36]. For Eu doped $CaSiO_3$ polycrystal, Eu^{3+} ion substitutes Ca^{2+} causing the crystal lattice distortion, since that Ca^{2+} and Eu^{3+} have different ionic radii [23] as can be seen in Fig. 2 (Eu^{3+} ion in yellow). Besides, there is a charge imbalance in the host lattice, produced by the doping of trivalent Eu^{3+} ion. Furthermore, Eu^{3+} ions in $CaSiO_3$ host can occupy interstitial sites, as a consequence, emitted light can be trapped in these sites decreasing the photoluminescence emission intensity [17, 23]. Nagabhushana et al. ([23]) have shown that the relative intensity of the emission lines of Eu^{3+} depends on the doping concentration of Eu^{3+} in the $CaSiO_3$ structure.

The excitation and emission spectra of unirradiated and irradiated $CaSiO_3$:Eu pellets are shown in Figs. 4 and 5, respectively. Exposure to an electron beam with the dose of 15 kGy (10 electron pulses) was performed, for each irradiation case.

Fig. 4 shows the excitation spectra in the broad wavelength in the range of 200–500 nm, monitored at the wavelength emission of 608 nm corresponding to the highest intensity of $^5D_0 \rightarrow {}^7F_2$ Eu^{3+} emission as shown in Fig. 5.

Excitation spectra were divided into two sections. Below 300 nm excitation spectra shows two broad excitation peaks and above 300 nm sharp $4f^6$–$4f^6$ electronic lines of Eu^{3+} ions as can be seen in Fig. 4. Due to these electronic lines have weaker intensity than those of the left side; a new re-scaling was made which is shown on the y-axis on the right. The left side shows the spectra in the middle ultraviolet region with one prominent excitation peak at 227.5 nm and another possible high intensity overlapping peak at 244.0 nm. These two overlapping contribution features in the UV region possibly coming from a different origin. Niraula et al. ([13]) have shown the excitation and emission spectra of the Eu^{3+} doped $CaSiO_3/SiO_2$ nanopowder. For emission spectra, no

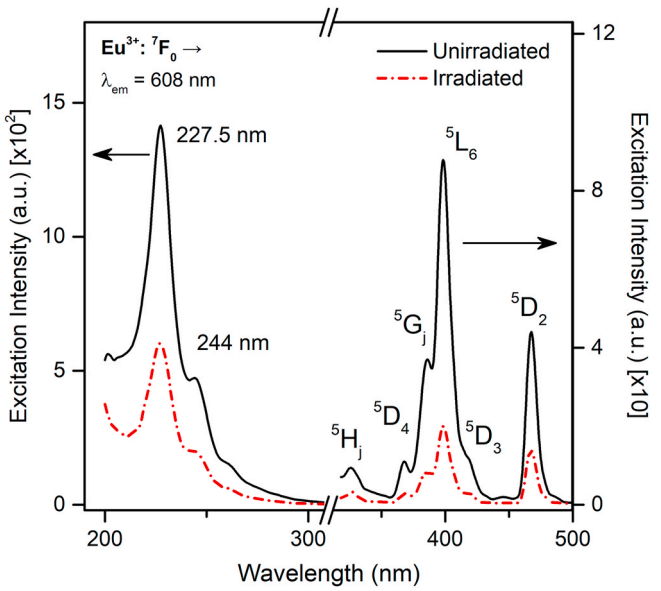

Fig. 4. PL excitation spectra of polycrystalline $CaSiO_3$:Eu for emission wavelength 608 nm. The solid line is for the unirradiated sample and the dash-dotted line for the irradiated sample at 15 kGy dose.

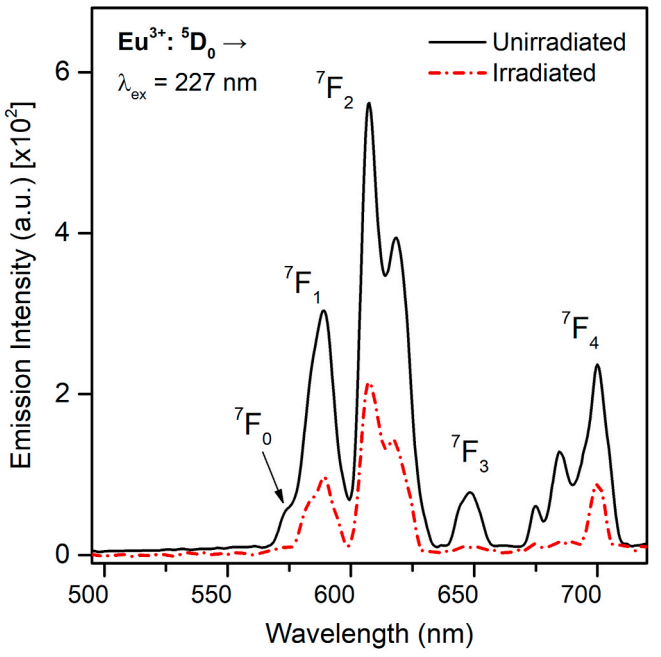

Fig. 5. PL emission spectra of polycrystalline $CaSiO_3$:Eu for excitation wavelength 227 nm. The solid line is for the unirradiated sample and the dash-dotted line for the irradiated sample at 15 kGy dose.

differences in the shape of these spectra have been found for both samples. However, when monitored at the wavelength emission of 610 nm, the excitation spectra of Eu^{3+} doped $CaSiO_3$ show one prominent peak at about 220 nm, and for Eu^{3+} doped SiO_2, two peaks at 220 and 223 nm have been found. In this work, similar two main peaks at the excitation spectra are shown as can be seen in Fig. 4. As mentioned by Niraula et al. ([13]), excitation spectra of Eu^{3+} doped phosphor are difficult to interpret since they depend largely on phase symmetry around the ion. On the other hand, Strzep et al. ([37]) have shown that the UV excitation feature in the sample of Eu^{3+}–doped $YAsO_4$ displays similar two overlapping contribution bands of different origins. The first one below 250 nm was produced by O^{2-}–Eu^{3+} charge transfer and the second at about 255 nm being assigned to O^{2-}–As^{5+} charge transfer occurring within the AsO_4^{3-} groups of the host lattice [23]. have explained that the excitation spectra of Eu doped $CaSiO_3$ consist mainly of a charge transfer band (CTB) of the Eu^{3+}-O^{2-} band in the short ultraviolet region (with a prominent band at about 250 nm). Furthermore [38], have explained that the broad band at 250 nm on the excitation spectra of CaO–SiO_2:0.01Eu^{3+} luminescent film (monitored at 616 nm) is attributed to charge transfer (CT) between the Eu^{3+} and the surrounding O^{2-} ions, whilst the lines are due to f–f transitions within the Eu^{3+} $4f^6$ configuration. The intensity of this CTB depends on the energy process efficiency from the CTB to the Eu^{3+} emitting level [38]. have shown that this efficiency increase with the increasing heat treatment temperature of the CaO–SiO_2:0.01Eu^{3+} luminescent films. That is, the interaction between O^{2-} and Eu^{3+} ions in the silicate host become stronger, whose reason could be due to that CTB of Eu^{3+}–O^{2-} shifts to lower energy.

On the basis of this consideration, it is suggested that the observed peak at 227.5 nm could be associated with CT transition from 2p orbital of O^{2-} to the incomplete 4f orbital of Eu^{3+} ions (O–Eu CT). Whilst the low energy shoulder at about 244.0 nm may be assigned to O^{2-}–Si^{4+} charge transfer (O–Si CT) occurring within the SiO_4^{4-} groups of the host lattice. However, further studies will be necessary to verify the different origins of these overlapping peaks, such as the change in the position of the O–Eu and O–Si bands with respect to the annealing temperature [37].

The sharp peaks shown at the right side of the excitation spectra shown in Fig. 4 are due to the intra 4f–4f transitions of Eu^{3+} ions as explained above. In this section, excitation spectra display six excitation bands of Eu^{3+} ions at 320.5, 364.0, 382.5, 395.5, 416.0 and 467.0 nm from $^7F_0$ ground state to ^5H_j, $^5D_4$, ^5G_j, $^5L_6$, $^5D_3$, and $^5D_2$ states, respectively. Among these transitions, the one corresponding to the electric dipole transition $^7F_0 \rightarrow {}^5L_6$ at 395.5 nm is the most intensity, while the magnetic dipole transition $^7F_0 \rightarrow {}^5D_{2,3,4}$, ^5G_j, and ^5H_j are the least intense [16,21,23,39]. These excitations at room temperature decay stepwise to the lowest excited $^5D_0$ level by a fast-nonradioactive relaxation, followed by a radiative transition to the o the ^7F_J ground state due to the large separation between $^5D_0$ and ^7F_j (J = 0,1,2,3,4) states. These radiative transitions are giving in the orange and red regions (530–730 nm) [17].

In Fig. 5 we can see the emission spectra in the broad wavelength region at the range of 530–730 nm, monitored at the wavelength excitation of 227.5 nm corresponding to the highest intensity of excitation spectra as can be seen in Fig. 4. Emission spectra shows five emission bands from the $4f^6$ electronic configuration of Eu^{3+} ions at 574.0, 589.0, 607.5, 648.5, and 700.0 nm which are attributed to the $^5D_0 \rightarrow {}^7F_J$ (J = 0,1,2,3,4) emission transitions, respectively. Similar emission spectra of the $CaSiO_3$:Eu^{3+} structure have been shown by Zhou et al. ([21]) when excited at an excitation wavelength of 393 nm. The $^5D_0 \rightarrow {}^7F_0$ transition is strictly forbidden according to the standard Judd–Ofelt theory [40]. This type of transition is a well-known example of the violation of the selection rules of the Judd-Ofelt theory [39]. The dipole character of this emission transition is the induced electric dipole (ED) transitions. The electric dipole transition comes from the interaction of the Eu ion with the electric field vector through an electric dipole. The creation of an electric dipole involves a linear movement of charge. This transition commonly appears at 570–585 nm wavelength range with a relative intensity between very weak to strong [39]. Besides, this transition is observed only for certain symmetries (C_n, C_{nv}, and C_s symmetry) indicating that the presence of this transition depends on the local environment [41]. From Fig. 5 although with very low intensity and overlapped with the $^5D_0 \rightarrow {}^7F_1$ transition, we can observe an emission band at about 574 nm which is ascribed to $^5D_0 \rightarrow {}^7F_0$ transition.

The $^5D_0 \rightarrow {}^7F_1$ transition is allowed as a magnetic dipole (MD) transition. An important feature of this transition is that its intensity is largely independent of the local symmetry of the Eu^{3+} ion [42]. The MD

transition is caused by the interaction of the lanthanide (europium) ion with the magnetic field component of light through a magnetic dipole. The appearance of the magnetic dipole supposes a curved movement of charge. Furthermore, MD transitions have a weak intensity comparable to those of induced electric dipole transitions [39]. This transition appears at about 585–600 nm wavelength range with a strong relativity intensity. In Fig. 5, the emission band at 589 nm is attributed to the $^5D_0 \rightarrow {}^7F_1$ transition.

The $^5D_0 \rightarrow {}^7F_2$ transition is also known as the "*hypersensitive transition*" because its luminescent intensity is much more influenced by the local symmetry of the Eu^{3+} ion and the nature of the ligands compared to the intensities of the other ED transitions [39]. This transition usually is characterized by a strong relative luminescence intensity and it usually appears between 610 and 630 nm [39]. In this case, for Eu doped $CaSiO_3$, the higher emission doublets at 607.5 and 618.5 nm are ascribed to $^5D_0 \rightarrow {}^7F_2$ as can be seen in Fig. 5. The splitting of the peaks shown in the emission spectra are attributed to the Stark effect, that is, the splitting of the energy levels by the crystal-field effect [39]. Therefore, the crystal field plays an important role in influencing the characteristics of the optical spectra as well as the Stark effect corresponding to the division of the energy levels of ions in solids [40].

Additionally, the weak intensity observed at 648.5 nm is ascribed to the ED $^5D_0 \rightarrow {}^7F_3$ transition, and the weak triplets observed at 648.5, 675.0, and 700.0 nm are associated with the ED $^5D_0 \rightarrow {}^7F_4$ transition.

As can be seen in Fig. 5, the emission intensity of the $^5D_0 \rightarrow {}^7F_2$ transition is stronger than that of the $^5D_0 \rightarrow {}^7F_1$ transition due to the Eu^{3+} ion in $CaSiO_3$ is located at the low or in non-centro symmetric sites [43]. It is assumed that the greater the symmetry of the rare earth ion site (e.g. Eu), the lower the intensity of the hypersensitive transitions. This is based on the fact that in theory, the intensity of the hypersensitive transition ($^5D_0 \rightarrow {}^7F_2$) is zero when the lanthanide ion is at a center of symmetry. This also occurs for the other induced ED transitions [44].

After all discussion of the results shown until now, a proposed electronic energy level diagram with the possible PL transition involved in this process is shown in Fig. 6. This figure was performed following the charge transfer band and energy level diagram of Eu^{3+} proposed by Nagabhushana et al. ([23]) and Strzep et al. ([37]). The left side shows the proposed O–Eu CT and O–Si CT transitions. The right side shows the excitation transition of Eu^{3+} ions. In this process, Eu^{3+} is raised to H, G, L, and D levels from the ground state. After that, Eu^{3+} ions decay non-radiatively (NR) to the $^5D_0$ level. Afterward, characteristics emission of Eu^{3+} ion occurs by a radioactive process.

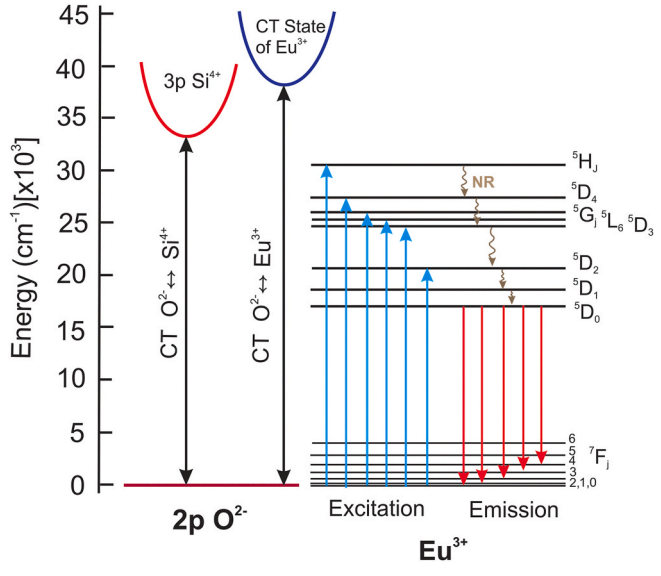

Fig. 6. Proposed electronic energy level diagram and PL transitions observed for Eu doped $CaSiO_3$ pellet.

As a consequence, it can be assumed that the main luminescence of Eu^{3+} belongs to pseudo-wollastonite. In tridymite, rare-earth ions are extremely poorly incorporated into the lattice. It is important to note here that the impurity Eu^{3+} segregates at the boundary of the tridymite phase, which can cause the effect of concentration quenching in this phase. Thus, the asymmetry of the Eu^{3+} photoluminescence signal is most likely due to the distortion of the nearest environment (1 coordination sphere), which stimulates the redistribution of the probabilities of radiative-nonradiative relaxation.

3.3. Electron irradiation effects

By comparing irradiation and unirradiated excitation spectra, all peaks are decreased about 60% at the left side and 75% at the right side without any changes in position as can be seen in Fig. 4. Besides, after pulsed electron irradiation dose of 15 kGy, emission intensities of all peaks have decreased by about 64% but keeping the same peak position and shape of the spectra. However, some transition intensities have almost disappeared such as the ED $^5D_0 \rightarrow {}^7F_0$ and $^5D_0 \rightarrow {}^7F_3$ transitions as shown in Fig. 5 (dash-dotted line). This decreased in photoluminescence intensities can be explained because the electron beam irradiation induces a higher efficiency of the $Eu^{3+} \rightarrow Eu^{2+}$ conversion process in the Eu^{3+}-doped $CaSiO_3$ polycrystal [9,10,45,46]. Moreover, the splitting effect in the $^5D_0 \rightarrow {}^7F_4$ transition has disappeared showing only the main peak at 700 nm. In this sense, $^5D_0 \rightarrow {}^7F_j$ (j = 0–4) transitions of the Eu^{3+} ion in the $CaSiO_3$ host is sensitive to electron beam irradiation.

Besides, there can be several other reasons for the decrease in the relative intensity of the Eu^{3+} luminescent signal: (a) since electrons are irradiated, a space charge (a certain internal electric field) arises in the matrix structure due to the spatial separation and localization of electrons and holes. Such a field distorts electronic transitions (material electrification effect) [47]. The energy of electrons during the used irradiation is insufficient for the formation of defects of a new type. Most likely, there is a recharge of the defects (intrinsic) present in the matrix, such as interstices or oxygen vacancies. (b) The sample is devitrified silicate. During devitrification, as a rule, defective micro-and nanocrystals are formed. When recharging, defects in nanocrystals distort structural units (oxygen octahedra, tetrahedra), including impurity Eu^{3+} ions. In this case, there is a change in the ratio of the probabilities of radiative and nonradiative transitions. (c) During devitrification, a small proportion of the residual glass phase is retained. Therefore, the non-single-phase nature of the samples under study can also be the reason for the redistribution of the intensity of the photoluminescent signal before and after exposure to accelerated electrons.

Malchukova and Boizot ([45]) have studied the $Eu^{3+} \rightarrow Eu^{2+}$ reduction in aluminoborosilicate (ABS) glasses under β-irradiation with 2.5 MeV electrons. They have shown that in this host the intensity ratio Eu^{2+}/Eu^{3+} as a function of Eu_2O_3 content decreased from 0.1 to 1.0 mol % of Eu_2O_3. That is, the increasing of Eu_2O_3 content in this glass material promotes the quenching of Eu^{2+} luminescence while the intensity of Eu^{3+} emission band is increasing. Moreover, the intensity of the broad and weak emission band due to Eu^{2+} ion (between 350 and 540 nm) in 0.2 mol% Eu_2O_3 doped of this ABS sample decreases as the excitation wavelength decreases. It is important to mention that Eu displays different luminescence characteristics according to its valence [14,16]. Eu^{3+} exhibits a red-light emission, while Eu^{2+} according to the host it may emit anywhere from UV to the deep red region [17,45,48,49]. Pandey and collaborators ([14]) have shown that Eu^{2+} peak of the photoluminescence spectra of the gamma-irradiated nanocrystalline $K_2Ca_2(SO_4)_3$:Eu is higher than that of the unirradiated sample. They concluded that it will be due to the $Eu^{3+} \rightarrow Eu^{2+}$ conversion as a result of irradiation. Pode and Dhoble [9] have shown that photoluminescence spectra of unirradiated YVO_4:Eu^{3+} shown a strong emission line of Eu^{3+} at 616, 594, and 575 nm due to $^5D_0 \rightarrow {}^7F_2$, $^5D_0 \rightarrow {}^7F_2$, and $^5D_0 \rightarrow {}^7F_2$ transitions respectively. However, when irradiated with gamma rays these emission lines are decreased without changes in the position.

Additionally, a broad and emission band at 425 nm is seen due to Eu^{2+} which is not observed in the unirradiated doped sample. They concluded that after gamma irradiation some of Eu^{3+} ions are converted into Eu^{2+} ions. These results are in good agreement with the fact of exposure to ionizing radiation of RE^{3+} (RE: rare earth) often it results in conversion $RE^{3+} \rightarrow RE^{2+}$ [46]. However, Zhu et al. ([10]) have shown that by comparing the luminescence spectra from the $^5D_0 \rightarrow {}^7F_j$ (j = 1–4) transitions in the Eu^{3+} ions of the Y_2O_3:Eu^{3+} phosphor is not sensitive to gamma irradiation. They argue that may be due to the shielding effect of the electrons in the 4f orbital by the outer 5s and 5p orbital for Eu^{3+} ions [10]. Upadeo and Moharil ([48]) have studied the radiation-induced valence changes in several Eu-doped phosphors. They have shown that the efficiency of $Eu^{3+} \rightarrow Eu^{2+}$ conversion is strongly dependent on the host material. They have concluded that (1) no $Eu^{3+} \rightarrow Eu^{2+}$ conversion was observed for compounds of La, Ga, and Y displaying a possible highly stabilized in the trivalent form in these compounds. (2) $Eu^{3+} \rightarrow Eu^{2+}$ conversion has been observed in several but not all phosphates, sulfates, and halides. Moreover, it has been observed that this conversion is greater for a lower concentration of Eu^{3+} (0.1–0.2 mol%.). That is, high Eu^{3+} concentration (a few moles per cent) could be adverse for radiation-induced $Eu^{3+} \rightarrow Eu^{2+}$ conversion [48]. Lim et al. ([50]) have studied the permanent $Eu^{3+} \rightarrow Eu^{2+}$ conversion in sodium borate glasses by irradiation of near-infrared femtosecond laser. They have shown that this conversion efficiency was dependent on the initial Eu^{3+} concentration, irradiation intensity, and exposure time. That is, this efficiency increased with the number of laser shots but decreased with a higher concentration of Eu^{3+} ions (in 0.05, 0.1, and 0.5 mol% glass samples).

In the present work no peaks, concerning Eu^{2+} ion have been observed between 400 and 560 nm in emission spectra of Eu^{3+} doped $CaSiO_3$ before and after electron beam irradiation dose of 15 kGy as can be seen in Fig. 5. This absence of peak could be because of the dopant quantity of Eu (1000 ppm) employed in the $CaSiO_3$ host and/or also due to the lower monitored excitation wavelength used (λ_{ex} = 227.5 nm). That is, the λ_{ex} used in this work could do not stimulate the typical emission Eu^{2+} due to the $4f^6 5\,d^1 - 4f^7$ transition [15]. However, in this work, we believe that there are no Eu^{2+} centers in the matrix under study, both before and after electron irradiation. Otherwise, strong luminescence in the blue-green spectral range would be observed, due to radiative d-f transitions with a high oscillator strength.

We are planning the PL study of Eu doped $CaSiO_3$ phosphor, doped at different quantities in ppm of Eu, and excited at different λ_{ex} values as a part of future works. We expect to know the relative intensity of Eu^{3+} emission bands according to different doping concentrations.

3.4. Symmetry of the crystal field around Eu^{3+}

Another probable fact found about the quenching effect on PL intensities can be because electron beam irradiation can induce the formation of defect centers in the $CaSiO_3$ host which acts as nonradiative recombination centers. Similar behavior has been reported by Buyanova et al. ([51]) for GaN material. They found that, after electron irradiation of this material, the quenching of PL intensity is possibly caused by the formation of deep-level centers that act as nonradiative recombination channels and/or optically active centers in the near-infrared spectral.

On the other hand, it is important to be mentioned that the variation of the site symmetry of Eu^{3+} ions in $CaSiO_3$ host can be evaluated from the evolution of the integrated emission intensity ratio of $^5D_0 \rightarrow {}^7F_2$ and $^5D_0 \rightarrow {}^7F_1$ transition also known as the asymmetric ratio R_{21} [22]. The High value of this asymmetry ratio indicates lower symmetry of the crystal field around Eu^{3+} ions [43,52].

In this work, the asymmetric ratio R_{21} has been calculated by considering the area under the electric dipole $^5D_0 \rightarrow {}^7F_2$ transition, divided by the area under the magnetic dipole $^5D_0 \rightarrow {}^7F_1$ transition for $CaSiO_3$:Eu polycrystal according to the analysis developed by Halappa et al. ([53]).

Asymmetric ratio R_{21} has been calculated for emission spectra of unirradiated and irradiated $CaSiO_3$:Eu. For this purpose, decomposition into Gaussians of the emission spectra as a function of energy (eV) was carried out to calculate the area below the emission curve. Fig. 7(a) and Fig. 7(b) show decomposition into Gaussians of the emission spectra for unirradiated and irradiated $CaSiO_3$:Eu, respectively (from Fig. 5).

The emission spectra shown in Fig. 7 (a) is composed of six Gaussians. Gaussians labeled with (1) and (2) corresponds to the $^5D_0 \rightarrow {}^7F_2$; (3), (4), and (5) to $^5D_0 \rightarrow {}^7F_1$; and (6) to $^5D_0 \rightarrow {}^7F_0$. Fig. 7(b) shows the decomposition into six Gaussian, (1), (2) and (3) corresponds to the $^5D_0 \rightarrow {}^7F_2$; (4), (5) and (6) to $^5D_0 \rightarrow {}^7F_1$. As explained before, for the unirradiated Eu doped $CaSiO_3$, the higher emission doublets at 607.5 and 618.5 nm are ascribed to $^5D_0 \rightarrow {}^7F_2$ (Fig. 5) which can be well resolved by two main Gaussians centered at 2.005 and 2.042 eV as shown in Table 1. The broad emission band at 589 nm which is attributed to the $^5D_0 \rightarrow {}^7F_1$ transition (Fig. 5) can be decomposed by three main Gaussians centered at 2.076, 2.099, and 2.121 eV (Table 1). Finally, the very low emission band at 574 nm (which is overlapped with the $^5D_0 \rightarrow {}^7F_1$ transition), ascribed to $^5D_0 \rightarrow {}^7F_0$ transition (Fig. 5) can be well resolved by one gaussian curve centered at 2.160 eV (Table 1). Similar analysis occurs for the electron irradiated Eu doped $CaSiO_3$, and reasons for the quenching photoluminescence after irradiation have been explained

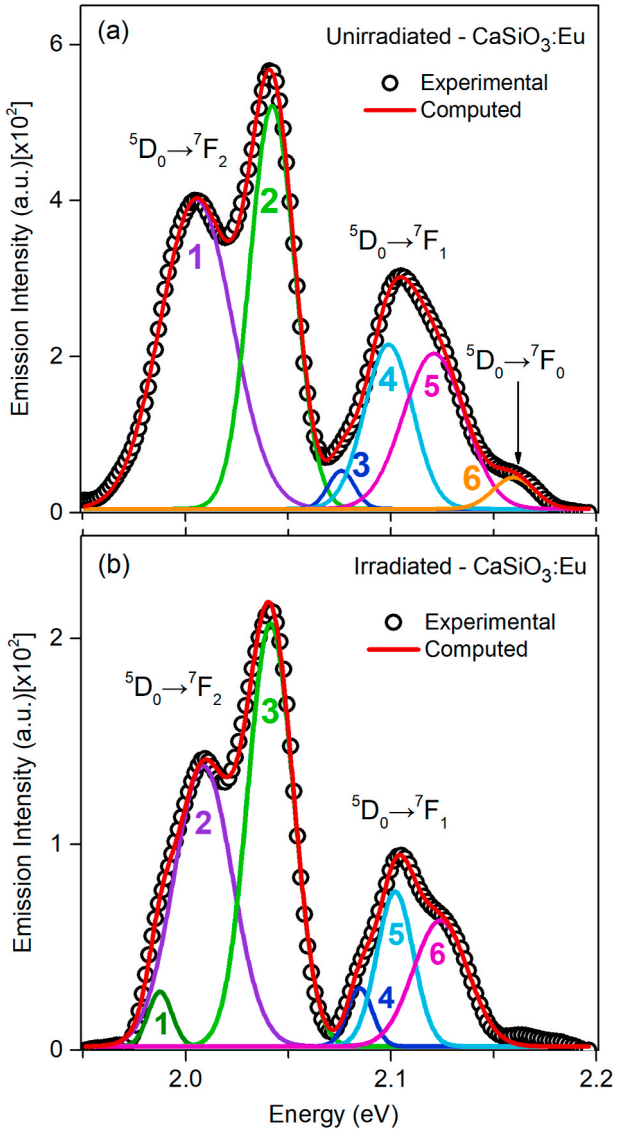

Fig. 7. Decomposition of emission spectra into Gaussian for $CaSiO_3$:Eu (a) before irradiation, and (b) after electron beam irradiation.

Table 1
Summary of Full half-width maximum (FWHM) and the position of maxima intensity (x_c) from Gaussians after emission spectra decomposition.

Gaussian number	Unirradiated		Irradiated	
	x_c (eV)	FWHM (eV)	x_c (eV)	FWHM (eV)
1	2.005	4.135×10^{-2}	1.987	1.369×10^{-2}
2	2.042	2.571×10^{-2}	2.009	3.362×10^{-2}
3	2.076	1.515×10^{-2}	2.041	2.606×10^{-2}
4	2.099	2.771×10^{-2}	2.085	1.459×10^{-2}
5	2.121	3.532×10^{-2}	2.102	2.096×10^{-2}
6	2.160	2.356×10^{-2}	2.124	3.136×10^{-2}

previously in this section.

As a result, the obtained asymmetric ratio for unirradiated $CaSiO_3$:Eu is $R_{21}(u) = 2.06$, and for irradiated $CaSiO_3$:Eu is $R_{21}(i) = 2.52$. It is possible to conclude that after electron beam exposure of this compound, there is a decrease in symmetry of the crystal field around Eu^{3+} ions due to its higher value of the asymmetric ratio R_{21} ($R_{21}(i) > R_{21}(u)$). R_{21} values for both the irradiated and non-irradiated cases are greater than 2 which indicates that the integrated emission intensity of transition $^5D_0 \rightarrow {}^7F_2$ is greater than twice that of transition $^5D_0 \rightarrow {}^7F_1$. Table 1 displays the summary of full half-width maximum (FWHM) and the position of maxima intensity (x_c) from Gaussians obtained after decomposition of the emission spectra for non-irradiated and irradiated $CaSiO_3$:Eu as shown in Fig. 7.

The study of luminescence optimization with a superior asymmetric ratio R_{21} has been the subject of several studies to obtain a pure red emission for optical applications [54,55]. Pure red emission is obtained from the $D_0 \rightarrow {}^7F_2$ emission transition of the $4f^6$ electronic configuration of Eu^{3+} ions, this transition being relatively strong if the symmetry of the crystal is low [53–55]. Yadav et al. ([56]), for instance, have found that a higher R_{21} value was obtained by the co-precipitation method used for the production of nano-size YBO_3:Eu^{3+} phosphor. In the present work, an improvement of the R_{21} is obtained after a high electron irradiation dose of 15 kGy in Eu doped $CaSiO_3$ compound.

4. Conclusions

Polycrystalline glass-ceramic Eu^{3+}-doped $CaSiO_3$ (1000 ppm) has been synthesized by the devitrification method. Powder pattern diffraction of this material has shown the main phase identified as pseudowollastonite (β-$CaSiO_3$) accompanied by a minor phase of tridymite (polymorphic of quartz - SiO_2).

The optical absorption of Eu^{3+}-doped $CaSiO_3$ shows an intense absorption band between 200 to 300 nm which is attributed to the oxygen to silicon (O–Si) LMCT in the SiO_4^{2-} group, and the broad-band between 300 to 500 is attributed to the intra configurational 4f →4f transitions from the $^7F_0$ level (excitation spectra). The induced broad visible band could be due to the formation of SiOHC or NBOHC centers.

Excitation spectra, monitored at 608 nm, shows one high-intensity excitation peak at 227.5 and an overlapping lower intensity peak at 244 nm. These peaks are possibly associated with O–Eu and O–Si CT transitions, respectively. Besides, the contribution of tridymite minority phase (SiO_2) could promote the O–Si CT process in the $CaSiO_3$:Eu sample.

Above 300 nm spectra display the characteristic excitation band of the Eu^{3+} ions, from $^7F_0$ ground state to ^5H_j (320.5 nm), $^5D_4$ (364 nm), ^5G_j (382.5 nm), $^5L_6$ (395.5 nm), $^5D_3$ (416 nm), and $^5D_2$ (467 nm) states. Among them, the electric dipole transition $^7F_0 \rightarrow {}^5L_6$ is the one with the most intensity.

Emission spectra, excited at 227 nm, exhibits the characteristics transition of Eu^{3+} ions in $CaSiO_3$ host corresponding to $^5D_0 \rightarrow {}^7F_0$ (574 nm), $^5D_0 \rightarrow {}^7F_1$ (589 nm), $^5D_0 \rightarrow {}^7F_2$ (607.5 and 618.5 nm), $^5D_0 \rightarrow {}^7F_3$ (648.5 nm), and $^5D_0 \rightarrow {}^7F_4$ (648.5, 675.0 and 700.0 nm). The splitting effect observed in $^5D_0 \rightarrow {}^7F_2$ and $^5D_0 \rightarrow {}^7F_4$ are attributed to the Stark effect. Moreover, the intensity of the $^5D_0 \rightarrow {}^7F_2$ transition is stronger than that of the $^5D_0 \rightarrow {}^7F_1$ transition due to the Eu^{3+} ion in $CaSiO_3$ is located at the low symmetric sites. A proposed electronic energy level diagram with the PL transition of Eu^{3+} ion in $CaSiO_3$ host has been performed.

After electron beam irradiation, all peaks of the PL spectra have decreased but maintaining the same peak position and shape. The decrease in the relative intensity of the Eu^{3+} can be due to the distortion of electronic transitions produced by the space charge originated in the electron irradiation. Besides, during the devitrification process defective micro-and nanocrystals are formed, that during irradiation, defects in nanocrystals distort structural units generating a change in the ratio of the probabilities of radiative and nonradiative transitions. Also, the non-single-phase nature of the samples under study can be the reason for the redistribution of the intensity of the photoluminescent signal before and after exposure to accelerated electrons.

The nonappearance of peaks regarding Eu^{2+} between 400 and 560 nm in emission spectra of Eu^{3+} doped $CaSiO_3$, before and after electron beam irradiation, could be because there are no Eu^{2+} centers in the matrix under study. That is, a strong luminescence in the blue-green spectral range due to radiative d-f transitions cannot be seen.

For the calculation of the asymmetric ratio R_{21} value, decomposition into Gaussians of the emission spectra as a function of energy (eV) was performed. The result shows a higher value of the R_{21} ratio found after electron beam irradiation ($R_{21}(i) = 2.52$). For the unirradiated case, it was found that asymmetric ratio $R_{21}(u) = 2.06$. These results indicate that there is a decrease in the symmetry of the crystal field around Eu^{3+} ions after irradiation. The improvement of the R_{21} obtained after high electron irradiation (about 18%) shows the luminescence optimization of Eu doped $CaSiO_3$ compound and its use in optical applications.

Declaration of competing interest

The authors declare that they have no known competing financial interests or personal relationships that could have appeared to influence the work reported in this paper.

Acknowledgments

This work was carried out with partial financial support from Fundação de Amparo à Pesquisa do Estado de São Paulo - FAPESP, Brazil (Process number 2014/03085–0). To Conselho Nacional de Desenvolvimento Científico e Tecnológico - CNPq, Brazil, for fellowship to C.D. Gonzales-Lorenzo (Process number 162741/2015–4). The authors would like to express our thanks to Dr. H. Loro from the National Engineering University (UNI), Peru, for allowing us to use the appropriate equipment for optical absorption measurements. Besides, C.D. Gonzales-Lorenzo kindly acknowledges the partial financial support from Consejo Nacional de Ciencia, Tecnología e Innovación Tecnológica (CONCYTEC) - Banco Mundial, through its executing unit FONDECYT, Peru (Process number 037-2019-FONDECYT-BM-INC.INV.). A.F. Zatsepin and A.N. Kiryakov were supported by the Russian Science Foundation (Grant N° 21-12-00392) and also the Russian Foundation for Basic Research-RFBR grants N° 20-42-660012.

References

[1] J. Qiu, Q. Jiao, D. Zhou, Z. Yang, Recent progress on upconversion luminescence enhancement in rare-earth-doped transparent glass-ceramics, J. Rare Earths 34 (2016) 341–367, https://doi.org/10.1016/S1002-0721(16)60034-0.
[2] P.P. Fedorov, A.A. Luginina, A.I. Popov, Transparent oxyfluoride glass ceramics, J. Fluor. Chem. 172 (2015) 22–50, https://doi.org/10.1016/j.jfluchem.2015.01.009.
[3] J. Zhong, D. Chen, Y. Peng, Y. Lu, X. Chen, X. Li, Z. Ji, A review on nanostructured glass ceramics for promising application in optical thermometry, J. Alloys Compd. 763 (2018) 34–48, https://doi.org/10.1016/j.jallcom.2018.05.348.
[4] H. Rahimian, H. Mokhtari, S.P. Pezhman Shirmardi, Improvement of Eu3+ emissions in oxyfluoride glass and nano glass-ceramic by electron beam irradiation, J. Lumin. 187 (2017) 535–539, https://doi.org/10.1016/j.jlumin.2017.03.025.

[5] K.I. White, K.J. Beales, J.E. Midwinter, G.R. Newns, Radiation effects on absorption losses in some optical glasses, Optoelectronics 6 (1974) 313–315, https://doi.org/10.1007/BF01423381.

[6] O. Gedeon, K. Jurek, I. Drbohlav, Changes in surface morphology of silicate glass induced by fast electron irradiation, J. Non-Cryst. Solids 353 (2007) 1946–1950, https://doi.org/10.1016/j.jnoncrysol.2007.01.058.

[7] S. Fakhfakh, B. Elsafi, Z. Fakhfakh, O. Jbara, Study of temperature effects on the conduction and trapping of charges in the alkali-silicate glass under electron beam irradiation, Appl. Surf. Sci. 258 (2012) 2324–2331, https://doi.org/10.1016/j.apsusc.2011.10.007.

[8] F.M. Nirwan, T.K. Gundu Rao, P.K. Gupta, R.B. Pode, Studies of defects in YVO_4: Pb^{2+}, Eu^{3+} red phosphor material, Phys. Status Solidi 198 (2003) 447–456, https://doi.org/10.1002/pssa.200306632.

[9] R.B. Pode, S.J. Dhoble, Radiation-induced defects in Eu^{3+}-activated yttrium vanadates, J. Phys. D Appl. Phys. 31 (1998) 146–150, https://doi.org/10.1088/0022-3727/31/1/018.

[10] C. Zhu, Y. Yang, G. Chen, S. Baccaro, A. Cecilia, M. Falconieri, Photoluminescence and gamma-ray irradiation of $SrAl_2O_4$:Eu^{2+} and Y_2O_3:Eu^{3+} phosphors, J. Phys. Chem. Solid. 68 (2007) 1721–1724, https://doi.org/10.1016/j.jpcs.2007.04.016.

[11] A. Kelemen, M. Ignatovych, V. Holovey, T. Vidóczy, P. Baranyai, Effect of irradiation on photoluminescence and optical absorption spectra of $Li_2B_4O_7$:Mn and $Li_2B_4O_7$:Ag single crystals, Radiat. Phys. Chem. 76 (2007) 1531–1534, https://doi.org/10.1016/j.radphyschem.2007.02.067.

[12] S. Sohal, M. Nazari, X. Zhang, E. Hassanzadeh, V. Kuryatkov, J. Chaudhuri, L. Hope-Weeks, J. Huang, M. Holtz, Effect of Tb^{3+} concentration on the optical and vibrational properties of YBO_3 tri-doped with Eu^{3+}, Ce^{3+}, and Tb^{3+}, J. Appl. Phys. 115 (2014) https://doi.org/10.1063/1.4875914, 183505.

[13] B.B. Niraula, C. Rizal, Photoluminescence property of Eu^{3+} doped $CaSiO_3$ nanophosphor with controlled grain size, Colloids Interfaces 2 (2018) 52, https://doi.org/10.3390/colloids2040052.

[14] A. Pandey, R.G. Sonkawade, P.D. Sahare, Thermoluminescence and photoluminescence characteristics of nanocrystalline $K_2Ca_2((SO)_4)_3$:Eu, J. Phys. D Appl. Phys. 35 (2002) 2744–2747, https://doi.org/10.1088/0022-3727/35/21/309.

[15] Q. Fei, C. Chang, D. Mao, Luminescent properties of $Sr_2MgSi_2O_7$ and $Ca_2MgSi_2O_7$ long lasting phosphors activated by Eu^{2+}, Dy^{3+}, J. Alloys Compd. 390 (2005) 133–137, https://doi.org/10.1016/j.jallcom.2004.06.096.

[16] J. Yang, L. Yang, W. Liu, Y. Zhang, H. Fan, Y. Wang, H. Liu, J. Lang, D. Wang, Luminescence behavior of Eu^{3+} in $CaSiO_3$:Eu^{3+}(Bi^{3+}) and Sr_2SiO_4:Eu^{3+}(Bi^{3+}), J. Alloys Compd. 454 (2008) 506–509, https://doi.org/10.1016/j.jallcom.2007.02.079.

[17] S.J. Dhoble, N.S. Dhoble, R.B. Pode, Preparation and characterization of Eu^{3+} activated $CaSiO_3$, (CaA)SiO_3 [A = Ba or Sr] phosphors, Bull. Mater. Sci. 26 (2003) 377–382, https://doi.org/10.1007/BF02711179.

[18] M. Madesh Kumar, R. Hari Krishna, B.M. Nagabhushana, C. Shivakumara, Synthesis, characterization and photoluminescence properties of Bi^{3+} co-doped $CaSiO_3$:Eu^{3+} nanophosphor, Spectrochim. Acta Mol. Biomol. Spectrosc. 139 (2015) 124–129, https://doi.org/10.1016/j.saa.2014.11.095.

[19] H. Xie, J. Lu, Y. Guan, Y. Huang, D. Wei, H.J. Seo, Abnormal reduction, $Eu^{3+} \rightarrow Eu^{2+}$, and defect centers in Eu^{3+}-doped pollucite, $CsAlSi_2O_6$, prepared in an oxidizing atmosphere, Inorg. Chem. 53 (2014) 827–834, https://doi.org/10.1021/ic402169w.

[20] C.D. Trinh, P.T. Pham Hau, T.M. Dung Dang, C.M. Dang, Sonochemical synthesis and properties of YVO_4:Eu^{3+} nanocrystals for luminescent security ink applications, J. Chem. (2019), https://doi.org/10.1155/2019/5749702, 2019, 5749702.

[21] L. Zhou, B. Yan, Sol–gel synthesis and photoluminescence of $CaSiO_3$:Eu^{3+} nanophosphors using novel silicate sources, J. Phys. Chem. Solid. 69 (2008) 2877–2882, https://doi.org/10.1016/j.jpcs.2008.07.012.

[22] Z. Andric, R. Krsmanovic, M. Marinovic-Cincovic, T. Dramicanin, B. Secerov, M. D. Dramicanin, Investigation on the crystallization process of Eu^{3+}:$CaSiO_3$ gel using optical and thermal methods, Acta Phys. Pol., A 112 (2007) 969–974, https://doi.org/10.12693/APhysPolA.112.969.

[23] H. Nagabhushana, B. Nagabhushana, M.M. Kumar, K. Murthy, C. Shivakumara, R. Chakradhar, Synthesis, characterization and photoluminescence properties of $CaSiO_3$:Eu^{3+} red phosphor, Spectrochim. Acta Part A Mol. Biomol. Spectr. 78 (2011) 64–69, https://doi.org/10.1016/j.saa.2010.08.063.

[24] C.D. Gonzales-Lorenzo, S. Watanabe, N.F. Cano, J.S. Ayala-Arenas, C.C. Bueno, Synthetic polycrystals of $CaSiO_3$ un-doped and Cd, B, Dy, Eu-doped for gamma and neutron detection, J. Lumin. 201 (2018) 5–10, https://doi.org/10.1016/j.jlumin.2018.04.037.

[25] C.D. Gonzales-Lorenzo, T.K. Gundu Rao, N.F. Cano, B.N. Silva-Carrera, R.R. Rocca, E.E. Cuevas-Arizaca, J.S. Ayala-Arenas, S. Watanabe, Thermoluminescence and defect centers in β-$CaSiO_3$ polycrystal, J. Lumin. 217 (2020), https://doi.org/10.1016/j.jlumin.2019.116783, 116783.

[26] C.D. Gonzales-Lorenzo, L.F. Nascimento, S. Kodaira, M.B. Gomes, S. Watanabe, Thermoluminescence studies of polycrystalline $CaSiO_3$ pellets for photons and particle therapy beams, Radiat. Phys. Chem. 177 (2020), https://doi.org/10.1016/j.radphyschem.2020.109132, 109132.

[27] Y. Nakanishi, A. Wakahara, H. Okada, A. Yoshida, T. Ohshima, H. Itoh, Effect of 3 MeV electron irradiation on the photoluminescence properties of Eu-doped GaN, Appl. Phys. Lett. 81 (2002) 1943–1945, https://doi.org/10.1063/1.1504873.

[28] T.K. Gupta, Radiation, Ionization, and Detection in Nuclear Medicine, Springer Berlin Heidelberg, 2013.

[29] M. Korzhik, G. Tamulaitis, A.N. Vasil'ev, Physics of Fast Processes in Scintillators, Springer Nature, 2020.

[30] D.V. Ananchenko, S.V. Nikiforov, S.F. Konev, G.R. Ramazanova, ESR and luminescent properties of anion-deficient α-Al2O3 single crystals after high-dose irradiation by a pulsed electron beam, Opt. Mater. 90 (2019) 118–122, https://doi.org/10.1016/j.optmat.2019.02.013.

[31] D.V. Sunitha, H. Nagabhushana, F. Singh, B.M. Nagabhushana, S.C. Sharma, R.P. S. Chakradhar, Thermo, Iono and photoluminescence properties of 100MeV Si^{7+} ions bombarded $CaSiO_3$:Eu^{3+} nanophosphor, J. Lumin. 132 (2012) 2065–2071, https://doi.org/10.1016/j.jlumin.2012.03.019.

[32] S.A. Speakman, Introduction to PANalytical X'Pert HighScore Plus v3.0, MIT Center for Materials Science and Engineering, 2012.

[33] T. Yamanaka, H. Mori, The structure and polytypes of α-$CaSiO_3$ (pseudowollastonite), Acta Crystallogr. B. 37 (1981) 1010–1017, https://doi.org/10.1107/S0567740881004962.

[34] Y.V. Seryotkin, E.V. Sokol, S.N. Kokh, Natural pseudowollastonite: crystal structure, associated minerals, and geological context, Lithos 134–135 (2012) 75–90, https://doi.org/10.1016/j.lithos.2011.12.010.

[35] H.A. ElBatal, M.Y. Hassaan, M.A. Fanny, M.M. Ibrahim, Optical and FT infrared absorption spectra of soda lime silicate glasses containing nano Fe_2O_3 and effects of gamma irradiation, Silicon 9 (2017) 511–517, https://doi.org/10.1007/s12633-014-9262-7.

[36] R.D. Shannon, Revised effective ionic radii and systematic studies of interatomic distances in halides and chalcogenides, Acta Crystallogr. A 32 (1976) 751–767, https://doi.org/10.1107/S0567739476001551.

[37] A. Strzep, A. Watras, K. Zawisza, P. Boutinaud, R.J. Wiglusz, Forgotten and resurrected chernovite-(Y): $YAsO_4$ doped with Eu^{3+} ions as a potential nanosized luminophore, Inorg. Chem. 56 (2017) 10914–10925, https://doi.org/10.1021/acs.inorgchem.7b01089.

[38] Q. Meng, J. Lin, L. Fu, H. Zhang, S. Wang, Y. Zhou, Sol–gel deposition of calcium silicate red-emitting luminescent films doped with Eu^{3+}, J. Mater. Chem. 11 (2001) 3382–3386, https://doi.org/10.1039/B105963G.

[39] K. Binnemans, Interpretation of europium (III) spectra, Coord. Chem. Rev. 295 (2015) 1–45, https://doi.org/10.1016/j.ccr.2015.02.015.

[40] B.M. Walsh, Judd-Ofelt theory: principles and practices, in: Advances in Spectroscopy for Lasers and Sensing, 2006, pp. 403–433, https://doi.org/10.1007/1-4020-4789-4_21.

[41] K. Binnemans, C. Görller-Walrand, Application of the Eu^{3+} ion for site symmetry determination, J. Rare Earths 14 (1996) 173–180.

[42] C. Görller-Walrand, L. Fluyt, A. Ceulemans, W.T. Carnall, Magnetic dipole transitions as standards for Judd–Ofelt parametrization in lanthanide spectra, J. Chem. Phys. 95 (1991) 3099–3106, https://doi.org/10.1063/1.460867.

[43] G. Jyothi, L.S. Kumari, K. Gopchandran, Site selective substitution and its influence on photoluminescence properties of $Sr_{0.8}Li_{0.2}Ti_{0.8}Nb_{0.2}O_3$:$Eu^{3+}$ phosphors, RSC Adv. 7 (2017) 28438–28451, https://doi.org/10.1039/C7RA03598E.

[44] C. Görller-Walrand, K. Binnemans, Chapter 167 Spectral intensities of f-f transitions, Handb. Phys. Chem. Rare Earths 25 (1998) 101–264, https://doi.org/10.1016/S0168-1273(98)25006-9.

[45] E. Malchukova, B. Boizot, Reduction of Eu^{3+} to Eu^{2+} in aluminoborosilicate glasses under ionizing radiation, Mater. Res. Bull. 45 (2010) 1299–1303, https://doi.org/10.1016/j.materresbull.2010.04.027.

[46] S.V. Moharil, S.V. Bodade, P.D. Sahare, S.M. Dhopte, P.L. Muthal, V.K. Kondawar, Luminescence in $LiNaSO_4$:Eu phosphor, Radiat. Eff. Defect Solid 127 (1993) 177–182, https://doi.org/10.1080/10420159308220313.

[47] R. Al-Obaidi, M. Wilke, M. Borgwardt, J. Metje, A. Moguilevski, N. Engel, D. Tolksdorf, A. Raheem, T. Kampen, S. Mähl, I. Yu Kiyan, E.F. Aziz, Ultrafast photoelectron spectroscopy of solutions: space-charge effect, New J. Phys. 17 (2015), https://doi.org/10.1088/1367-2630/17/9/093016, 093016.

[48] S.V. Upadeo, S.V. Moharil, Radiation-induced valence changes in Eu-doped phosphors, J. Phys. Condens. Matter 9 (1997) 735–746, https://doi.org/10.1088/0953-8984/9/3/013.

[49] M.I. Danilkin, A.P. Belousov, S.O. Klimonskii, V.D. Kuznetsov, A.L. Lust, V. N. Nikiforov, L.N. Paama, I.Kh Pammo, V.O. Seeman, Formation of Eu^{2+} and Eu^{3+} centers in synthesis of CaF_2:Eu luminophores, J. Appl. Spectrosc. 74 (2007) 858–865, https://doi.org/10.1007/s10812-007-0133-5.

[50] K.S. Lim, S. Lee, M.T. Trinh, S.H. Kim, M. Lee, D.S. Hamilton, G.N. Gibson, Femtosecond laser-induced reduction in Eu-doped sodium borate glasses, J. Lumin. 122–123 (2007) 14–16, https://doi.org/10.1016/j.jlumin.2006.01.067.

[51] I.A. Buyanova, Mt Wagner, W.M. Chen, B. Monemar, J.L. Lindström, H. Amano, I. Akasaki, Photoluminescence of GaN: effect of electron irradiation, Appl. Phys. Lett. 73 (1998) 2968–2970, https://doi.org/10.1063/1.122646.

[52] M.M. Yawalkar, G.D. Zade, K.V. Dabre, S.J. Dhoble, Luminescence study of Eu^{3+} doped $Li_6Y(BO_3)_3$ phosphor for solid-state lighting, Luminescence 31 (2016) 1037–1042, https://doi.org/10.1002/bio.3006.

[53] P. Halappa, B. Devakumar, C. Shivakumara, Effect of Ca^{2+} ion co-doping on radiative properties via tuning the local symmetry around the Eu^{3+} ions in orange red light emitting $GdPO_4$:Eu^{3+} phosphors, New J. Chem. 43 (2019) 63–71, https://doi.org/10.1039/C8NJ04372H.

[54] U. Rambabu, S.D. Han, Luminescence optimization with superior asymmetric ratio (red/orange) and color purity of MBO_3:Eu^{3+}@SiO_2 (M = Y, Gd and Al) nano down-conversion phosphors, RSC Adv. 3 (2013) 1368–1379, https://doi.org/10.1039/C2RA21304D.

[55] Y. Wang, L. Wang, Photoluminescence properties of $Y_{0.95-x}M_xBO_3$:Eu_{3+} (M=Ca, Sr, Ba, Zn, Al, $0 \leq x \leq 0.1$) in 100–450 nm regions, Mater. Lett. 60 (2006) 2645–2649, https://doi.org/10.1016/j.matlet.2006.01.056.

[56] R.S. Yadav, R.K. Dutta, M. Kumar, A.C. Pandey, Improved color purity in nano-size Eu^{3+}-doped YBO_3 red phosphor, J. Lumin. 129 (2009) 1078–1082, https://doi.org/10.1016/j.jlumin.2009.04.032.